Fluoride and Formate Interaction with Liver and Erythrocyte Catalases as Revealed by Solvent–Proton Magnetic Relaxation†

S. Vuk-Pavlović*,‡ and D. L. Williams-Smith§

ABSTRACT: The temperature dependence of solvent proton magnetic relaxation rates in solutions of bovine liver and human erythrocyte catalases has been determined for the native enzymes and in the presence of formate, fluoride, and formate + fluoride. A significant enhancement of proton magnetic relaxation (^{1}H NMR) rates occurred on addition of fluoride. From the frequency dependence of ^{1}H NMR rates, the correlation time for the iron–electron and proton dipole–dipole interaction, τ_c, was calculated together with possible numbers of exchanging protons which closely approach the heme iron and their corresponding nuclear–electron interspin distances. These data were not consistent with the hypothesis that the protons of a water molecule at the sixth coordination position of the iron could account for the observed ^{1}H NMR rates. In solutions of catalase in the presence of both formate and fluoride, these rates were higher than in catalase–formate. In the former solution electron paramagnetic resonance measurements demonstrated that fluoride did not directly bind heme iron, unlike catalase in the presence of fluoride alone. It is concluded that the major contribution to the observed ^{1}H NMR rates comes from rapidly exchangeable protons outside the axial coordination positions of heme iron and that fluoride increases the number and/or decreases the interspin distances of such protons, probably via conformational and/or hydration changes in the catalase protein rather than directly by binding catalase heme.

Solvent–proton magnetic relaxation (^{1}H NMR[1]) enhancement in solutions of paramagnetic metalloproteins has yielded information about the stereochemistry of the immediate neighborhood of the paramagnetic centers and about the mechanisms and stoichiometry of formation of higher macromolecular complexes (Mildvan and Cohn, 1970). While the results obtained in manganese containing protein complexes can usually be interpreted with great accuracy (Mildvan and Cohn, 1970; Lanir et al., 1975), the interpretation of ^{1}H NMR data in solutions of ferric hemoproteins is particularly complex due in part to ambiguities regarding the applicability of either of the two proposed stereochemical models for the mechanism of magnetic relaxation of the nuclear spins of the solvent molecules.

While one of the models (Maričić et al., 1966) is based on the assumption of the exchange of water (or protons) between the sixth coordination site of the ferric ion and the bulk of the solvent, the alternative (Pifat et al., 1973) assumes (for ferric hemoglobin) a water molecule exchanging with the bulk of the solvent from a site next to the axial ligand site; here the exchange of the liganded water is assumed to be too slow to appreciably affect the ^{1}H NMR rates of the protons in the solvent. Recently several papers have been published which describe the use of changes in ^{1}H NMR enhancement to study the location of ligand binding sites in horseradish peroxidase (Lanir and Schejter, 1975; Schejter et al., 1976) and liver catalase (Hershberg and Chance, 1975; Lanir and Schejter, 1976). The results were interpreted on the basis of the first model, i.e., assuming a profound role for the axially liganded water in the observed ^{1}H NMR effects. For horseradish peroxidase it was subsequently shown that the interpretation of the same data according to the second model (Pifat et al., 1973) is at least equally self-consistent (Vuk-Pavlović and Benko, 1975).

It has been suggested from indirect evidence that catalase has a water molecule at the sixth (axial) coordination position of its heme iron (Nicholls and Schonbaum, 1963; Deisseroth and Dounce, 1970). Hershberg and Chance (1975) and Lanir and Schejter (1976) interpreted their data on the basis of this water molecule being the major contributor to the observed ^{1}H NMR rates (i.e., they adopted the first of the described models). In addition, the latter authors considered that ligands such as formate, which at high concentrations decreased the observed ^{1}H NMR rates, displaced this water molecule.

The aim of this paper is to discuss the applicability of these two models to the interpretation of ^{1}H NMR data in the solutions of variously liganded bovine liver and human erythrocyte catalases. Our experimental data are sufficient to discriminate between them and can also demonstrate some stereochemical relations between the ions and small molecules which interact with the enzyme; these relations are essential to an understanding of catalase function.

Experimental Section

Bovine liver catalase, two times crystallized, was obtained from the Sigma Chemical Co. Ltd., type C-100. Crystals were dissolved by extensive dialysis against 20 mM phosphate, 5×10^{-4} M EDTA, 0.1 M NaCl, pH 7.0. Human erythrocyte catalase was isolated by the method of Saha et al. (1964) and was finally purified on Whatman DE 52 and Sephadex G-150.

The ratios of maxima in the electronic spectra were $A_{405}/A_{280} = 0.87$ for the bovine sample and $A_{405}/A_{280} = 1.02$ for the human enzyme.

The electron paramagnetic resonance (EPR) spectrum of bovine liver catalase showed iron contaminants at $g = 8.5, 2.9,$

† From the Macromolecular Biophysics Laboratory, Institute of Immunology, Rockefellerova 2, 41000 Zagreb, Croatia, Yugoslavia (S.V.-P.), and the Department of Physics, Guy's Hospital Medical School, London Bridge, London, SE1 9RT, England (D.L.W.-S.). *Received March 23, 1977.*

‡ Supported by the U.S. P.L. 480 Grant 02-004-1 between N.I.H. and the Institute of Immunology, Zagreb, Yugoslavia. The final version of this paper was prepared while holding a long-term fellowship from the European Molecular Biology Organization at the Department of Chemical Immunology, The Weizmann Institute of Science, Rehovot, Israel.

§ Supported by the Cancer Research Campaign.

[1] Abbreviations used are: ^{1}H NMR, proton magnetic relaxation; EPR, electron paramagnetic resonance.

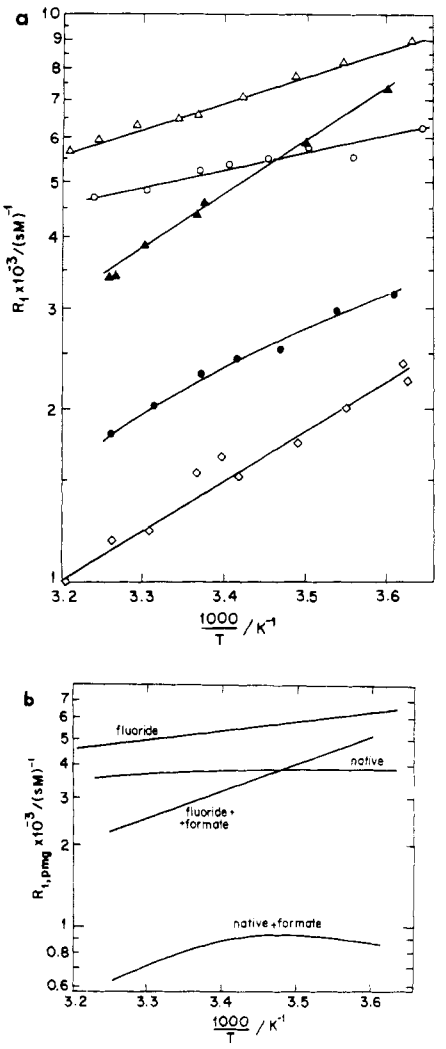

FIGURE 1: (a) The molar (per heme) solvent-proton longitudinal magnetic relaxation rates measured at 24 MHz in solutions of bovine liver catalase in 0.1 M NaCl, 20 mM phosphate, 5×10^{-4} M EDTA, pH 7.0. Concentration of the heme was between 0.2 and 0.3 mM. (○) Native enzyme; (●) formate (150 mM); (△) fluoride (100 mM); (▲) fluoride (100 mM) + formate (150 mM); (◇) carbonmonoxy reduced. (b) The molar (per heme) paramagnetically induced ^{1}H NMR rates derived from data in (a) by subtraction of the ^{1}H NMR rates of CO-reduced sample from the corresponding paramagnetic derivative.

1.5 and $g = 4.3$. The former signal represents 35 ± 5% of the number of spins in the active catalase heme component, $g = 6.5$, 5.4, 2.0 (for a discussion of the identity of these signals, see Williams-Smith and Patel, 1975). This calculation was performed by double integrating computer simulations of the line shapes of the two species (Aasa and Vänngård, 1975) and assumes the same percentage population of the lowest Kramer's doublets of these species at 4.2 K, an approximation we feel is justified by the similarity of the temperature dependence of the signal intensities of the two species between 4.2 and 20 K (D.L. Williams-Smith, unpublished observations). Erythrocyte catalase is free of the $g = 8.5$ signal and the $g = 4.3$ signal in this preparation has an intensity, relative to the $g = 6.5$ signal, of only 10% of the relative intensity of this signal in the liver catalase.

The solutions of formate and sodium fluoride were added from freshly prepared buffered stock solutions. The concentrations of catalase in samples were determined photometrically using the extinction coefficient at 405 nm per heme of 1.485×10^5 cm^{-1} M^{-1} for the liver enzyme (Deisseroth and Dounce, 1967) and 9.5×10^4 cm^{-1} M^{-1} for erythrocyte catalase (Nicholls and Schonbaum, 1963).

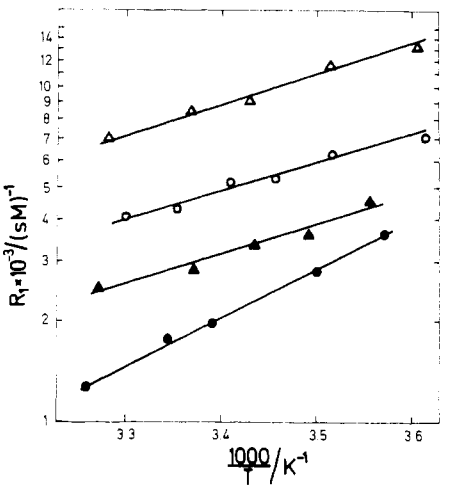

FIGURE 2: The molar (per heme) ^{1}H NMR rates measured in solutions of human erythrocyte catalase under the same conditions as in Figure 1a. The symbols represent the analogous derivatives as in Figure 1a.

The carbonmonoxy derivative of the bovine enzyme was prepared by reduction of the ferric enzyme with sodium dithionite under a stream of carbon monoxide. The solution of the enzyme was frozen in liquid nitrogen and thawed several times prior to reduction (Dounce and Howland, 1943). It has been estimated that after such a reduction procedure up to 10% of the catalase molecules may still be oxidized (Dounce and Schwalenberg, 1950).

The temperature dependence of the solvent-proton longitudinal magnetic relaxation times, T_1, in solutions of variously liganded catalase was measured at 24 MHz by the π-t-$\pi/2$ pulse sequence using a pulse spectrometer built at Jožef Stefan Institute, Ljubljana, Yugoslavia, and a high resolution Bruker BE-40-A-magnet, as described previously (Vuk-Pavlović et al., 1974). The measurements at 5.4, 12.0, and 37.4 MHz were performed by the same pulse sequence at 24 °C. EPR spectra were obtained with a Varian Associates E9 spectrometer operating at X band (~9.2 GHz). Samples were cooled to 4.2 K using an Oxford Instrument Co. Ltd. liquid helium cryostat.

Results and Discussion

Determination of Longitudinal Relaxation Rates and Their Temperature Dependence. Plots of the logarithms of the molar (per heme) solvent proton magnetic relaxation rates vs. reciprocal absolute temperature are presented in Figure 1a for bovine liver catalase solutions, and in Figure 2 for human erythrocyte catalase. The molar relaxation rates (both for paramagnetic and diamagnetic derivatives) were obtained by subtracting the ^{1}H NMR rate measured for the protein-free buffer (this value has been found to be independent of added fluoride and formate) and dividing by the concentration of the heme; they are influenced both by the interaction of the solvent-protons with the diamagnetic protein matrix as well as with the large magnetic moment of the high-spin ferric iron:

$$R_1 = R_1(\text{paramagnetic}) + R_1(\text{diamagnetic}) \qquad (1)$$

Since the structural information about the vicinity of the metal ion is obtained from the paramagnetic term in eq 1, the diamagnetic one had to be measured independently and subtracted from the R_1 value. This contribution to R_1 was measured in the diamagnetic ferrous carbonmonoxy derivative.

The purely paramagnetically induced molar ^1H NMR rates for the bovine enzyme are presented in Figure 1b. According to the accepted model of solvent-nuclei magnetic relaxation in dilute solutions of paramagnetic ions (Swift and Connick, 1962; Luz and Meiboom, 1964), the type of temperature dependence of the ^1H NMR rates is given by:

$$R_{1,pmg} = (1/T_1N)_{pmg} = \frac{n}{N_w} \frac{1}{\tau_M + T_{1M}} \quad (2)$$

where n denotes the number of protons within the "sphere of closest approach" as defined by Pifat et al. (1973) which may or may not be identical with a ligand site within the first coordination sphere. N stands for the molarity of paramagnetic species and N_w for the concentration of solvent-protons, uncorrected for the volume occupied by the enzyme itself due to its low concentration in our samples. τ_M is the residence time of a nucleus at the "site of closest approach" where it relaxes with a characteristic relaxation time T_{1M}. When $\tau_M > T_{1M}$ it is expected that the molar relaxation rates will increase with increasing temperature, when $\tau_M \ll T_{1M}$ then it is found that they decrease with increasing temperature (Luz and Meiboom, 1964).

In full accord with the data reported by Lanir and Schejter (1976) in neutral solutions of the native enzymes (Figures 1 and 2) the fast-exchange mechanism is operative, $\tau_M \ll T_{1M}$ (eq 2). This can be concluded from the temperature dependence and the absolute values of the molar relaxation rates in Figures 1a, b and 2.

Solutions of both bovine liver and human erythrocyte enzymes show a similar temperature dependence of their ^1H NMR rates and similar changes on addition of fluoride and formate. Although the observed molar ^1H NMR rates are higher in erythrocyte catalase, it would appear that the interpretation of these rates in bovine liver catalase is not obscured by the presence of significant amounts of iron contaminants at $g_x = 8.5$ and $g = 4.3$.

^1H NMR in Solutions of Catalase-Fluoride. ^1H NMR rates in solutions of catalase fluoride are presented in Figures 1a, b and 2. As can be seen, these rates are higher than in the native enzymes, an effect also observed in some other heme proteins (Vuk-Pavlović, 1976). From the temperature dependence it can be seen that the fast exchange mechanism is again operative. EPR measurement on the human erythrocyte catalase preparation (Figure 3) shows a ^{19}F hyperfine interaction at g_z of 4.2 mT, and considerable broadening of the g_x, g_y lines. This interaction is of a similar magnitude to that in other heme proteins, e.g., methemoglobin, 4.4 mT, and it must be concluded that fluoride is bound directly at an axial coordination position of catalase heme.

Both catalase and catalase fluoride show significant rhombicity (7.2 ± 0.2%, 7.9 ± 0.5%) in their EPR spectra, unlike metmyoglobin (0.2%) and its fluoride complex (0.88%) (Peisach et al., 1971). In cytochrome P450 it has been shown that such rhombicity could arise via asymmetric electronic interactions with an appropriate axial ligand, in this case mercaptide sulfur where on mixing in of the p_x, p_z sulfur lone pair orbitals the $p_x(p_y)$ can overlap with the iron $d_{xz}(d_{yz})$ orbitals to effectively remove the degeneracy of the d_{xz} and d_{yz} orbitals, with loss of axial electronic symmetry at the iron (Hanson et al., 1977). If, as we suspect, such a model is applicable to catalase, then on the basis of the EPR data in catalase and metmyoglobin and their fluorides it must be concluded that the fifth (axial) ligand is retained in catalase-fluoride. It then follows, providing the heme iron is six coordinate, that fluoride binds the sixth coordination position to displace the (presumed) bound water molecule. This should result in a diminution of the ^1H NMR rates, contrary to the observed increase on binding fluoride if, as assumed by both Hershberg and Chance (1975) and Lanir and Schejter (1976), the protons of this water molecule were largely responsible for the observed relaxation rates. In attempting to predict the effects of fluoride binding on the observed ^1H NMR rates it should be noted that the pH dependence of the binding of fluoride, and other ligands—such as formate, azide, and acetate—indicate that they bind to the free acids (Chance, 1952).

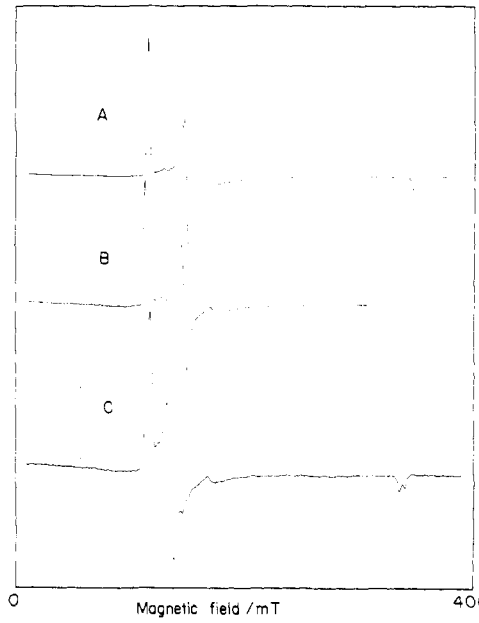

FIGURE 3: EPR spectra at 4.2 K of human erythrocyte catalase derivatives in 0.25 M Hepes, pH 7.0, at 9.167 GHz. (A) Formate (100 mM); (B) formate (100 mM) + fluoride (100 mM); (C) fluoride (100 mM).

In two peroxidases, horseradish peroxidase and lactoperoxidase, the kinetics of fluoride binding have been studied in detail. In the first case the pH dependence of binding was accounted for by fluoride binding to protonated horseradish peroxidase (Dunford and Alberty, 1967), in the second the kinetic evidence favored lactoperoxidase binding free hydrofluoric acid (Segal et al., 1968). In either mechanism two protons close to the heme would be replaced by only one, and in these peroxidases the kinetics of binding and dissociation are slow, thus, by analogy, exchange mechanisms involving protonated fluoride are considered highly unlikely in catalase.

^1H NMR in Solutions of Catalase-Formate in the Presence of Fluoride. The temperature dependences of the molar ^1H NMR rates both of fluoride complexes and native enzymes with bound formate are given in Figures 1a,b and 2.

The addition of 150 mM formate decreases the molar paramagnetic ^1H NMR rates in native catalase from both sources. An increase in the relaxation rate is then obtained on addition of 100 mM fluoride to catalase formate. Since an increase in ^1H NMR rate also resulted from addition of fluoride to the native enzyme, this might be interpreted as indicating that in solutions of catalase-formate fluoride binds directly at the heme iron.

However, EPR spectra at 4.2 K of human erythrocyte catalase in the presence of fluoride (100 or 200 mM) and formate (100 or 50 mM) are identical with those of catalase-formate (Figure 3). No ^{19}F hyperfine splitting at g_z or broadening at g_x, g_y is observed. Furthermore, optical titrations of catalase-fluoride vs. formate at room temperature show the pres-

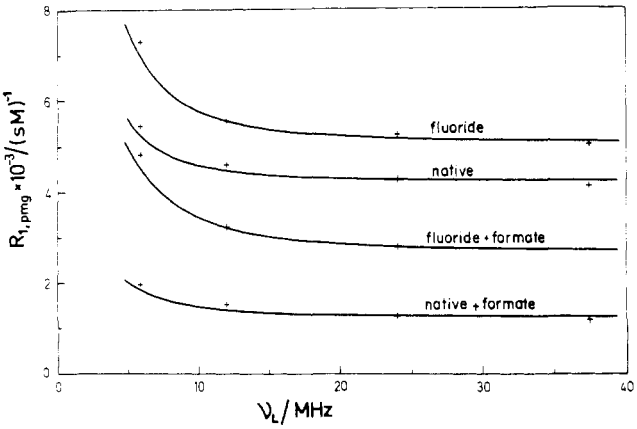

FIGURE 4: The frequency dependence of the paramagnetically induced molar (per heme) ^{1}H NMR rates in the solutions of bovine liver catalase derivatives measured at 24 °C. Other conditions as in Figure 1a. The lines are computer best-fits obtained under conditions described in the text.

ence of only two spectral components, catalase-formate and catalase fluoride. In solutions 100 mM in fluoride, catalase-formate is exclusively formed at formate concentrations of >50 mM, pH 7.0. Thus, one can observe fluoride-induced enhancements of ^{1}H NMR rates even when fluoride is not directly bound to catalase heme. It should, however, be noted that in the formate/fluoride solutions the proton relaxation rates are not as great as in the native enzymes, or in catalase-fluoride. Also, it should be noted that the anisotropy in the effective g tensor of the iron is unchanged in solutions of catalase-formate/fluoride at these concentrations. Hence this fluoride induced enhancement of ^{1}H NMR rates cannot be due to major electronic changes of the iron.

Possible Proton-Iron Interspin Distances. Since the fast-exchange condition is fulfilled both in the solutions of the native enzyme and fluoride complexes, the theory (Solomon, 1955) enables one to calculate the effective correlation times for the dipole-dipole interaction of the iron-electron and proton spins, τ_c, from the frequency dispersion data.

The simplified form of Solomon's (1955) equation is applicable since $\omega_I^2\tau_c^2 \ll 1$ and $\omega_s \gg \omega_I$:

$$1/T_{1M} = B[3\tau_c + 7\tau_c/(1 + \omega_s^2\tau_c^2)] \quad (3)$$

B equals $2\gamma_I^2 g^2 \mu_B^2 S(S + 1)/15r^6$. Here γ_I stands for the proton gyromagnetic ratio, g is the electronic g factor, μ_B is the Bohr magneton, S is the total electronic spin ($S = 5/2$ for the high-spin ferric hemoproteins), and r is the electron-nucleus interspin distance. τ_c is the characteristic time of the modulation of the fluctuating local magnetic fields on the nuclear spin (correlation time) and ω_I and ω_S are the Larmor frequencies of the nuclear and electronic precession. As shown on several occasions for the solutions of high spin ferric hemoglobin and myoglobin, the actual correlation time, τ_c, is the longitudinal electronic relaxation time of the heme iron, τ_s (Lahajnar et al., 1974, 1976; Lanir and Schejter, 1976).

Keeping n in eq 2 and B in eq 3 constant (Lahajnar et al., 1974) and using the frequency dispersion data presented in Figure 4, a nonlinear regression computer program (Smolej, 1973) yielded the correlation times of 1.19×10^{-10} s for the native enzyme, 9.3×10^{-11} s for the fluoride, 7.9×10^{-11} s for the formate, and 6.2×10^{-11} s for the formate + fluoride complex.

In Table I are presented computations, using eq 2 and 3, of the numbers of protons and the iron-proton interspin distances which would be required to account for the observed ^{1}H NMR rates in the solutions of native and fluoro derivative of liver

TABLE I: The Values of Proton-Electron Interspin Distances, r, Calculated for Different Numbers of Protons Taking Part in the Fast-Exchange Mechanism, n, in Bovine Liver Catalase Solutions.[a]

n	Interspin distance, r (Å), of derivatives	
	Native	Fluoride
1	2.50	2.25
2	2.80	2.57
4	3.15	2.88
6	3.37	3.08

[a] Calculated from eq 2 and 3 using the purely paramagnetically induced ^{1}H NMR rates at 24 °C (Figure 1b) and correlation times given in the text.

enzyme. In these calculations the outer-sphere contributions to the ^{1}H NMR rates were not subtracted from the paramagnetically induced relaxation rates, and g tensor anisotropy has been neglected (Sternlicht, 1965). It is not expected that these simplifications would markedly affect our general conclusions. Since both native enzyme and fluoride complex are in the high-spin state (Nicholls and Schonbaum, 1963; Torii et al., 1970), one would expect a decrease of the paramagnetically induced ^{1}H NMR rates upon replacement of the (putative) water by fluoride, if it really were this water molecule responsible for the most of the ^{1}H NMR effect in the native enzyme too. Even if by such a ligand replacement the electron-proton interspin distance is not altered, the ^{1}H NMR rates in fluoride complex would decrease due to the shortening of the correlation time and to a slight decrease of the magnetic moment (Torii et al., 1970). However, this is contrary to our experimental data (Figures 1 and 2).

In the case of leghemoglobin (Vuk-Pavlović et al., 1976) and horseradish peroxidase (Vuk-Pavlović and Benko, 1975), the interspin distances in solutions of both aquo and fluoro ferric derivatives are very similar, generally being longer than 4 Å. Therefore, on the basis of these expected values, the model which proposes a dominant role for the HF proton in the ^{1}H NMR effect appears unlikely, since our ^{1}H NMR measurements indicate that this proton should exchange with the bulk solvent from a site as close to the iron as some 2.3 Å (Table I). This value is also considerably shorter than the water-proton to iron distance of 2.84 Å estimated from x-ray data of other heme proteins (Lanir and Schejter, 1976).

The Mechanism of Solvent-Proton Magnetic Relaxation Enhancement. The consideration of the mechanisms of the ^{1}H NMR rates in solutions of catalase derivatives is based on two assumptions. The first of these is the applicability of the Solomon-Bloembergen equations. In line with objections listed by Dwek (1973), Lanir and Schejter (1976) have thoroughly analyzed these equations with regard to the present system. They have shown that the evaluation of correlation times from the frequency dispersion data is not straightforward due to a large zero-field splitting in high-spin ferric hemoproteins. Also, deviation from the rapid tumbling conditions, $\tau_s \gg \tau_R$, where τ_R is the rotational correlation time, introduces an uncertainty which depends on the actual value of the zero-field splitting parameter in the given complex (Doddrell et al., 1976). Accurate numerical analysis of data according to the theory of Pegg and Doddrell (1976) would require precise values of T_M. These values cannot be derived here unequivocally due to the unknown number of protons actually participating in the exchange mechanism (n in eq 2). However, electronic parameters of the catalase hemes do not change much upon binding of fluoride (Torii and Ogura, 1968), and conclusions based on relative changes are thus justified, irrespective of the theory

TABLE II: The Line Widths of the g_x EPR Lines in Single Heme Peroxidases and Catalases at 4.2 K.[a]

Enzyme derivative	g_x	$\Delta H_{1/2}$ (mT)
Lactoperoxidase	6.40	3.85
Lactoperoxidase fluoride	6.33	3.75
Horseradish peroxidase fluoride	6.36	4.40
Human erythrocyte catalase	6.50	2.27
Bovine liver catalase	6.50	4.30
Bovine liver catalase fluoride	6.56	6.06
Rat liver catalase	6.50	3.00

[a] Full experimental details will be published elsewhere.

adopted. Therefore, although we do not insist on a high reliability of the calculated values of τ_c's, the *relative* changes of this parameter upon binding of fluoride and/or formate as reflected in calculated interspin distances are very indicative. The discrepancy between the expected diminution and observed increase of the ^{1}H NMR rates upon binding of fluoride to the native enzyme (vide supra) demonstrates that the putative sixth coordinated water molecule is of no importance for the ^{1}H NMR mechanism. Here this conclusion can be reached with certainty, since, in both the native enzyme and fluoride derivative, the same, fast exchange ^{1}H NMR mechanism is operative.

The second assumption is that the paramagnetic heme irons can be treated as point-dipoles in a very dilute solution. Recently Waysbort and Navon (1975) and Lanir et al. (1975) have shown that delocalization of the electronic spin onto the orbitals of the ligand may result in an increase of the effective magnetic moment of the paramagnetic center, which, in turn, may enhance the ^{1}H NMR rates. Such an effect is also possible in the present series of catalase derivatives. In addition, Maeda et al. (1973) have proposed on the basis of their Mossbauer data the existence of two different Fe-Fe distances in catalase tetramer, in one pair of hemes this being as small as about 7 Å, so that the point-dipole approximation may not be applicable. Such a proposed structure with two adjacent hemes is consistent with the hypothesis of Deisseroth and Dounce (1970) that the catalatic reaction might require the second hydrogen peroxide molecule to be bound at a second heme, in close proximity to the first.

However, there is not yet any EPR evidence for such heme-heme structures. The line widths of 4.2 K in catalase are of the same order as those in single heme peroxidases (Table II). These line widths are a little variable, in bovine liver catalase ± 0.4 mT, probably due to the presence of a distribution of heme environments, rather than heme-heme interactions. The line shapes of catalase are easily computer simulated using procedures which do not include electron spin-electron spin interactions between neighboring paramagnets and are similar to single hemoproteins which have the appropriate rhombic distortions. Furthermore, the temperature dependence of the EPR intensity of bovine liver catalase between 4.2 and 20 K shows no sharp changes in intensity in this region, such as might occur if there was antiferromagnetic coupling of the right magnitude (D. L. Williams-Smith, unpublished observations).

From the preceding arguments concerning the ligand environment of catalase, the increase in ^{1}H NMR rate on binding fluoride, and the calculated interspin distances, we conclude that the hypothesis that a water molecule coordinated at the sixth (axial) coordination site of heme iron is largely responsible for the observed ^{1}H NMR rates is untenable.

The site from which the exchanging species communicates with the bulk of the solvent is therefore not given by the coordination properties of the iron, but by the stereochemistry of its immediate neighborhood. As shown in Table I, at least six protons approaching the iron to about 3 Å in the fluoride complex of bovine enzyme are needed to explain the high ^{1}H NMR rates. Since we have shown for the native enzyme that the axial ligand does not take a major part in the ^{1}H NMR mechanism, it is plausible that more than two protons simultaneously approach the iron to distances longer than 3 Å in the native enzyme, too. This is compatible with a high accessibility of the heme for solvent molecules.

Such an "open" heme environment is perhaps necessary in the peroxidative reactions to properly accommodate the hydrogen donors with respect to the activated peroxide, and to permit the extremely fast rate of the catalatic reaction. Similar structural conclusions were derived from ^{1}H NMR data in horseradish peroxidase solutions (Vuk-Pavlović and Benko, 1975).

At high concentrations of formate, higher than those required to effect optical and EPR changes in catalase heme (Chance, 1952; Williams-Smith and Patel, 1975; Lanir and Schejter, 1976), the ^{1}H NMR rate is lowered due to displacement of protons in the heme neighborhood. When fluoride is then added to such solutions, the ^{1}H NMR rate is again enhanced as a result of protein conformation and/or hydration changes which either increase the number of protons near the heme or reduce the iron-proton distances (or both). Although we have shown that a rigorous quantitative evaluation is not possible, in no case will the protons of the putative axially coordinated water greatly affect the observed ^{1}H NMR rates. The possible displacement of this water molecule from the sixth coordination position should not be inferred from changes in ^{1}H NMR rates.

Acknowledgments

We would like to thank Mrs. K. Patel for skilled technical assistance and Mr. V. Smolej for the calculation of correlation times, Dr. S. Maričić and Professor S. J. Wyard for helpful discussions, advice, and encouragement, Dr. S. Wherland for reading, and Ms. Z. Cohen for typing the manuscript.

References

Aasa, R., and Vänngård, T. (1975), *J. Magn. Reson. 19,* 308-315.

Chance, B. (1952), *J. Biol. Chem. 194,* 483-496.

Deisseroth, A., and Dounce, A. L. (1967), *Arch. Biochem. Biophys. 120,* 671-692.

Deisseroth, A., and Dounce, A. L. (1970), *Physiol. Rev. 50,* 319-375.

Doddrell, D. M., Bendall, M. R., and Gregson, A. R. (1976), *Aust. J. Chem. 29,* 55-64.

Dounce, A. L., and Howland, J. W. (1943), *Science 97,* 21-23.

Dounce, A. L., and Schwalenberg, R. R. (1950), *Science 111,* 654-655.

Dunford, H. B., and Alberty, R. A. (1967), *Biochemistry 6,* 447-451.

Dwek, R. A. (1973), Nuclear Magnetic Resonance in Biochemistry: Application to Enzyme Systems, Oxford, Clarendon Press, pp 179-180.

Gupta, R. K., and Mildvan, A. S. (1975), *J. Biol. Chem. 250,* 246-253.

Hanson, L. K., Sligar, S. G., and Gunsalus, I. C. (1977), *Croat. Chem. Acta 49,* 237-250.

Hershberg, R., and Chance, B. (1975), *Biochemistry 14,* 3885-3891.

Lahajnar, G., Benko, B., Rutar, V., and Zupančič, I. (1976), *Int. J. Pept. Protein Res. 8,* 317–322.
Lahajnar, G., Zupančič, I., Blinc, R., Pifat, G., and Maričić, S. (1974), *Biopolymers 13,* 1187–1193.
Lanir, A., Gradstajn, S., and Navon, G. (1975), *Biochemistry 14,* 242–248.
Lanir, A., and Schejter, A. (1975), *Biochem. Biophys. Res. Commun. 62,* 199–203.
Lanir, A., and Schejter, A. (1976), *Biochemistry 15,* 2590–2596.
Luz, Z., and Meiboom, S. (1964), *J. Chem. Phys. 40,* 2686–2692.
Maeda, Y., Trautwein, A., Gonser, U., Yoshida, K., Kikuchi-Torii, K., Homma, T., and Ogura, Y. (1973), *Biochim. Biophys. Acta 303,* 230–236.
Maričić, S., Ravilly, A., and Mildvan, A. S. (1966), In Hemes and Hemoproteins, Chance, B., Estabrook, R. W., and Yonetani, T., Ed., New York, N.Y., Academic Press, pp 157–172.
Mildvan, A. S., and Cohn, M. (1970), *Adv. Enzymol. 33,* 1–70.
Nicholls, P., and Schonbaum, G. R. (1963), *Enzymes, 2nd Ed. 8,* 147–225.
Pegg, D. T., and Doddrell, D. M. (1976), *Aust. J. Chem. 29,* 1869–1884.
Peisach, J., Blumberg, W. E., Ogawa, S., Rachmilewitz, E. A., and Oltzik, R. (1971), *J. Biol. Chem. 246,* 3342–3355.
Pifat, G., Maričić, S., and Grandja, S. (1973), *Biopolymers 12,* 905–920.
Saha, A., Campbell, D. H., and Schroeder, W. A. (1964), *Biochim. Biophys. Acta 85,* 38–49.
Schejter, A., Lanir, A., and Epstein, N. (1976), *Arch. Biochem. Biophys. 174,* 36–44.
Segal, R., Dunford, H. B., and Morrison, M. (1968), *Can. J. Biochem. 46,* 1471–1474.
Smolej, V. (1973), Delovno Poročilo, Jožef Stefan Institute, Ljubljana, Yugoslavia.
Solomon, I. (1955), *Phys. Rev. 99,* 559–565.
Sternlicht, H. (1965), *J. Chem. Phys. 42,* 2250–2251.
Swift, T. J., and Connick, R. E. (1962), *J. Chem. Phys. 37,* 307–320.
Torii, K., Iizuka, T., and Ogura, Y. (1970), *J. Biochem. (Tokyo) 68,* 837–841.
Torii, K., and Ogura, Y. (1968), *J. Biochem. (Tokyo) 64,* 171–179.
Vuk-Pavlović, S., and Benko, B. (1975), *Biochem. Biophys. Res. Commun. 66,* 1154–1159.
Vuk-Pavlović, S., Benko, B., and Maričić, S. (1974), *Biophys. Chem. 2,* 359–368.
Vuk-Pavlović, S., Benko, B., Maričić, S., Lahajnar, G., Kuranova, I. P., and Vainshtein, B. K. (1976), *Int. J. Pept. Protein Res. 8,* 427–434.
Waysbort, D., and Navon, G. (1975), *J. Chem. Phys. 62,* 1021–1026.
Williams-Smith, D. L., and Patel, K. (1975), *Biochim. Biophys. Acta 405,* 243–252.

Mechanism of the Prenyl-Transfer Reaction. Studies with (*E*)- and (*Z*)-3-Trifluoromethyl-2-buten-1-yl Pyrophosphate†

C. Dale Poulter*,‡ and Dennis M. Satterwhite

ABSTRACT: The prenyl-transfer reaction catalyzed by porcine farnesyl pyrophosphate synthetase has been studied using (*E*)- and (*Z*)-3-trifluoromethyl-2-buten-1-yl pyrophosphates as substrates and inhibitors. The rate of condensation between isopentenyl pyrophosphate (IPP) and the allylic fluoro analogues is drastically depressed relative to the normal catalytic rate observed with dimethylallyl pyrophosphate (DMAPP) or geranyl pyrophosphate (GPP). A similar depression is found in the rates of solvolysis for methanesulfonate derivatives of the fluoro analogues in aqueous actone under typical SN1 reaction conditions. Prolonged incubation of [^{14}C]IPP and (*E*)- or (*Z*)-CF_3-DMAPP with the enzyme, followed by treatment with alkaline phosphatase, gave a product that comigrated with geranylgeraniol on a polystyrene column. Both fluoro analogues showed mixed linear inhibition patterns with DMAPP or GPP as the variable substrate. We interpret these results in terms of an ionization–condensation–elimination mechanism for the prenyl-transfer reaction.

Prenyltransferase (EC 2.5.1.1) catalyzes the condensation between C_1 of an allylic pyrophosphate and C_4 of isopentenyl pyrophosphate (IPP),[1] yielding the five-carbon homologue of the allylic pyrophosphate. This is the basic polymerization reaction in the terpene biosynthetic pathway and leads to such diverse classes of natural products as sterols, dolichols, carotenoids, respiratory coenzymes, and a multitude of plant terpenoids. The mechanisms which have been proposed for the prenyl-transfer reaction can be grouped into two broad catagories (see Scheme I): those in which condensation is initiated by a heterolytic cleavage of the carbon–oxygen bond of the allylic pyrophosphate, with or without anchimeric assis-

† From the Department of Chemistry, University of Utah, Salt Lake City, Utah 84112. *Received April 15, 1977.* This investigation was supported by Research Grant GM 21328 from the National Institutes of Health.

‡ Alfred P. Sloan Fellow; Career Development Award from the National Institutes of Health, HL 00084, 1975–1980.

[1] Abbreviations used are: IPP, isopentenyl pyrophosphate; DMAPP, dimethylallyl pyrophosphate; CF_3-DMAPP, 3-trifluoromethyl-2-buten-1-yl pyrophosphate or trifluoromethyldimethylallyl pyrophosphate; GPP, geranyl pyrophosphate; FPP, farnesyl pyrophosphate; GGPP, geranylgeranyl pyrophosphate; NMR, nuclear magnetic resonance; UV, ultraviolet; IR, infrared; Me_4Si, tetramethylsilane; DSS, sodium 4,4-dimethyl-4-silapentanesulfonate; GLPC, gas–liquid phase chromatography.